

Partitioning of preferential flows in fracture networks:

Smoothed Particle Dynamics simulations and analytical modeling of infiltration dynamics

EGU 2020, Mai 2020

Jannes Kordilla¹, Marco Dentz², Alexandre Tartakovsky³

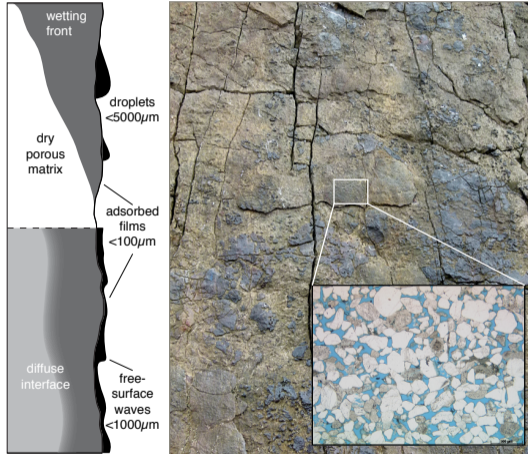
¹University of Goettingen, Applied Geosciences, Goettingen, Germany

²PNNL, Richland, USA

³IDAEA (CSIC), Barcelona, Spain

Preferential flow in porous-fractured media

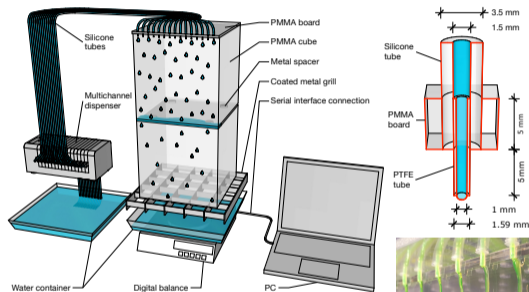
Fracture scales: Overview



- Scales: mm vs. μm
- Breakdown of classical volume-effective approaches
- Challenging: Rapid and erratic flow dynamics
- Flowrate dependent flow modes: Droplets \rightarrow rivulets \rightarrow films
- Common force balance: **viscous** $<$ **inertial** $<$ **capillary**
- Apertures above $\sim 0.8\text{mm}$: Transition into inertial regime (Wood et al 2005, WRR)

What is happening at fracture intersections?

Analogue percolation experiments



- Total flow rate $Q_0 = 15 \text{ ml/min}$
- Flow regimes: Droplet flow ($15 \times 1 \text{ ml/min}$) and rivulet flow ($3 \times 5 \text{ ml/min}$)
- Cascade of cubes: $20 \text{ cm} \times 20 \text{ cm} \times 20 \text{ cm}$
- Aperture width $d_f = 1 \text{ mm}$ and 2.5 mm
- Static contact angle $\theta_0 \approx 65^\circ$

Laboratory setup (Kordilla et al. 2017, Noffz et al. 2018)

Fracture inflow:
$$Q_f(t) \equiv \frac{dM_f(t)}{dt} = Q_0 - \frac{dM_b(t)}{dt} \quad (1)$$

Washburn:
$$\frac{dl(t)}{dt} = \frac{c_f}{l(t)} \quad c_f = \frac{\Delta P_c}{\mu} \frac{d_f^2}{4} \quad (2)$$

Parallel plate :
$$\Delta P = \frac{2\sigma \cos(\theta)}{d_f} \quad (3)$$

$$l(t = t_0) = l_0 \quad l(t) = \sqrt{l_0^2 + 2c_f(t - t_0)}. \quad (4)$$

$$M_f(t) = A_f l(t) \quad Q_f(t) = A_f \frac{dl(t)}{dt} = \frac{Q_0}{\sqrt{1 + 2k_f(t - t_0)}} \quad (5)$$

$$k_f = c_f / l_0^2 \quad (6)$$

Regime transitions

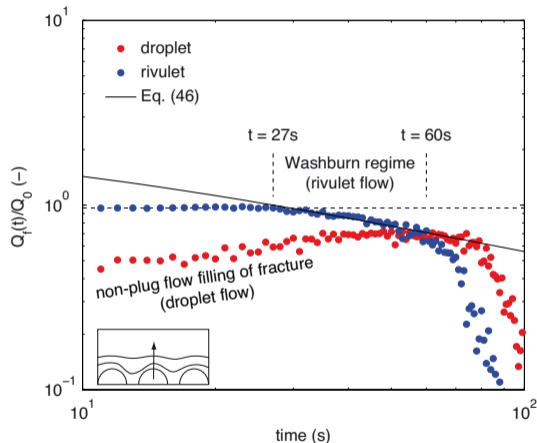


Figure 1: Kordilla et al. (2017)

- Both boundary conditions: Recovery of classical Washburn $t^{-1/2}$ scaling
- Transition times depend on intersection partitioning dynamics
- Rivulet flow: Initially rapid plug flow filling of horizontal fracture, then transition into Washburn regime
- Droplet flow: Individual droplets bypass until fluid front is closed. Transition into Washburn regime occurs later

What about “upscaling”?

Transfer-function

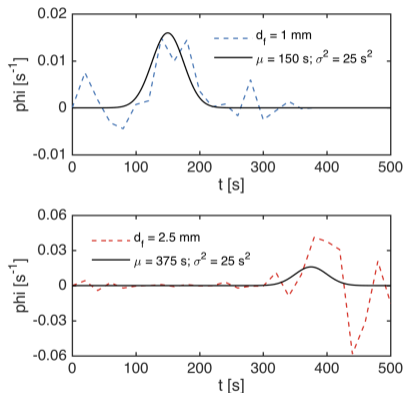


Figure 2: Transfer function φ vs. time (Noffz et al. 2018).

Output signal:

$$Q_{nf}(t) = \int_0^t \varphi_{nf}(t-t') Q_{nf-1}(t')$$

Transfer-function:

$$\varphi(t) = \frac{dQ_1(t)}{dt} = -\frac{dQ_f(t)}{dt}$$

Gaussian:

$$\varphi(t) \propto \frac{\exp\left[-\frac{(t-\mu)^2}{2\sigma^2}\right]}{\sqrt{2\pi\sigma^2}}$$

$$\int_0^\infty dt \varphi(t) = 1$$

Inflow:

$$Q_{f,nf}(t) = Q_0 \left[1 - \int_0^t dt_{nf-1} \varphi(t-t_{nf-1}) \dots \right]$$

$$\int_0^{t_3} dt_2 \varphi(t_3-t_2) \int_0^{t_2} dt_1 \varphi(t_1) \Big]_5$$

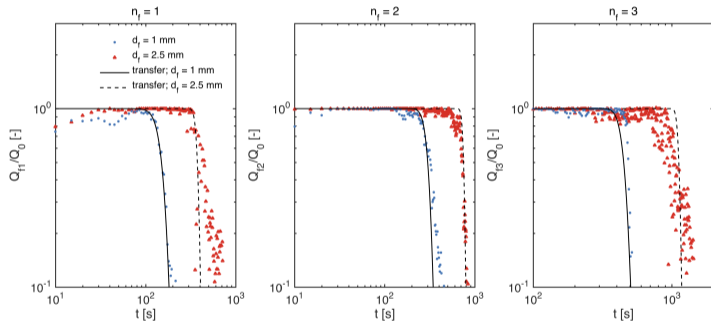


Figure 3: Normalized fracture inflow rate vs. time (Noffz et al. 2018).

- Predictive modeling of unsaturated flow dynamics during rivulet flow by Gaussian transfer-function
- Better recovery of tailing requires better process understanding

Can we parameterize $\varphi(\dots)$ to model the outflow?

Process-based transfer function

$$\varphi_{pw}(t) = \frac{1}{Q_0} \frac{dQ}{dt} = \delta(t_c - t) - \frac{W(t)a}{Q_0} [\delta(t - t_{max}) - \delta(t - t_c)] + \frac{W'(t)a}{Q_0} [\mathcal{H}(t - t_{max}) - \mathcal{H}(t - t_c)]$$

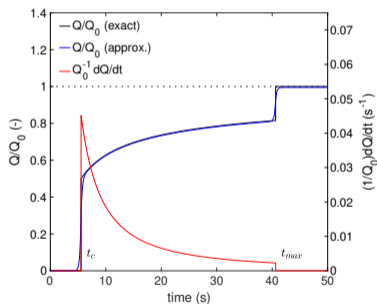


Figure 4: Normalized outflow rate and transfer function $\varphi_{pw}(t) = Q_0^{-1}dQ/dt$ (Kordilla et al. 2020, under revision).

- Process-based normalized outflow via an analytical approach
- Transfer function takes into account the switch from plug-flow to Washburn-type flow at a critical time t_c
- W is a Washburn-type penetration function applied to a horizontal fracture with aperture a

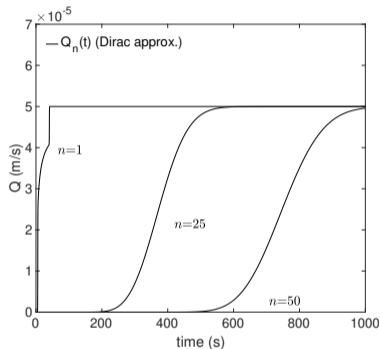


Figure 5: Flow through a system of $n = 1, 25$ and 50 fractures and $L_{max} = 0.3$ m where $t_{max} > t_c$ (Kordilla et al. 2020, under revision).

- Modeling of outflow through a system of n fracture intersections

$$Q_n(t) = \int_0^t Q_{n-1}(t') \varphi_{pw,p}(t - t') dt' \quad (7)$$

- Simple yet effective analytical approach
- Applicable to systems with low matrix porosity and/or short time-scales
- Effect of porous matrix imbibition not yet included

What about the porous matrix?

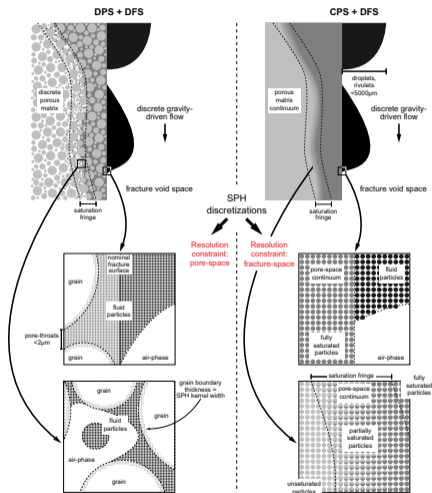


Figure 6: Multiscale SPH coupling scheme (Kordilla 2017)

Governing Equations

$$\text{Navier-Stokes equation: } \frac{d\mathbf{v}}{dt} = -\frac{1}{\rho} \nabla P + \frac{\mu}{\rho} \nabla^2 \mathbf{v} + \mathbf{g}$$

$$\text{Richards equation: } \frac{\partial \Theta(\psi)}{\partial t} = (C_m + \rho \mathbf{g} S_e S_s) \frac{\partial \psi}{\partial t} = \nabla \cdot \mathbf{K}_s k_r(\psi) \nabla \psi + \frac{\partial K(\psi)}{\partial z}$$

Van Genuchten Parameters:

$$\left. \begin{aligned} S_e &= \frac{1}{[1 + |\alpha \psi^n|]^m} \\ \Theta &= \Theta_r + S_e (\Theta_s - \Theta_r) \\ k_r &= S_e^l \left[1 - \left(1 - S_e^{\frac{1}{m}} \right)^m \right]^2 \\ C_m &= \frac{\alpha m}{1-m} (\Theta_s - \Theta_r) S_e^{\frac{1}{m}} \left(1 - S_e^{\frac{1}{m}} \right)^m \end{aligned} \right\} \text{if } \psi < 0$$
$$\left. \begin{aligned} S_e &= 1.0 \\ \Theta &= \Theta_s \\ k_r &= 1.0 \\ C_m &= 0.0 \end{aligned} \right\} \text{if } \psi \geq 0$$

SPH - discretization of Navier-Stokes equation:

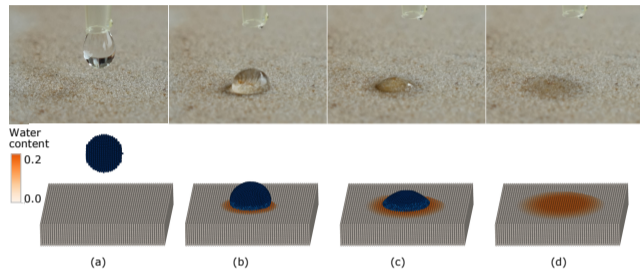
$$\frac{d\mathbf{v}_i}{dt} = - \sum_{j=1}^N m_j \left(\frac{P_j}{\rho_j^2} + \frac{P_i}{\rho_i^2} \right) \frac{\mathbf{r}_{ij}}{r_{ij}} \cdot \frac{dW(r_{ij}, h)}{dr_{ij}} + 2\mu \sum_{j=1}^N m_j \frac{\mathbf{v}_{ij}}{\rho_i \rho_j r_{ij}} \cdot \frac{dW(r_{ij}, h)}{dr_{ij}} +$$

$$\mathbf{g} + \frac{1}{m_i} \sum_{j=1}^N s_{ij} \left(A_{ij} \tilde{W}(r_{ij}, \frac{h}{2}) \frac{\mathbf{r}_{ij}}{r_{ij}} - \tilde{W}(r_{ij}, h) \frac{\mathbf{r}_{ij}}{r_{ij}} \right)$$

SPH - discretization of Richards equation:

$$\frac{d\Theta_i}{dt} = (C_{m_i} + \rho_i \mathbf{g} S e_i S_i) \frac{d\psi_i}{dt} = \sum_{j=1}^N 2 \frac{m_i m_j}{m_i + m_j} \frac{\rho_i + \rho_j}{\rho_i \rho_j} \cdot \mathbf{K}_s k_{r_i} (d\psi_{ij} + dz_{ij}) \cdot \frac{dW(r_{ij}, h)}{dr_{ij}}$$

Droplet infiltration



The experimental (top) and simulation (bottom) results of droplet imbibition at different times: (a) $t_0 = -0.004$ s, (b) $t_1 = 0.396$ s, (c) $t_2 = 1.836$ s, and (d) $t_3 = 2.676$ s (Shigorina et al. 2020, under revision).

- Saturation of solid by water particles (no penetration)
- Water particles are removed if their virtual saturation falls below critical threshold

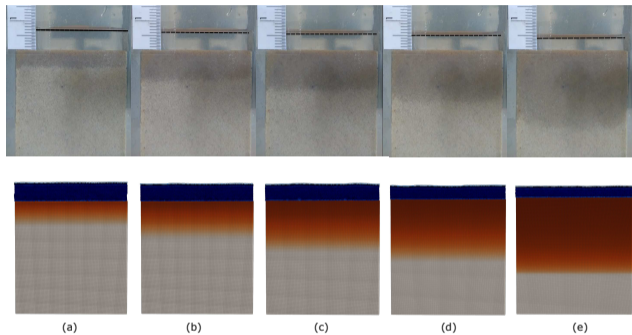
- Mass conservation:

$$\frac{\partial \Theta}{\partial t} = \nabla \cdot (\sum q_{in} - \sum q_{out}) = 0$$

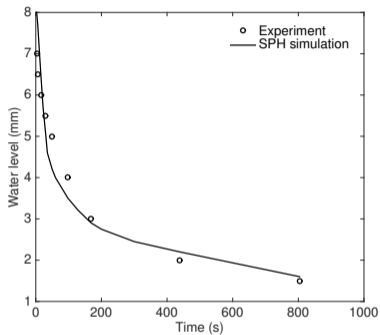
- Total water content:

$$\Theta_{total} = const$$

Validation experiment



Experimental (top) and simulation (bottom) results of infiltration into a sandstone: (a) $t_1 = 3$ s; (b) $t_2 = 16$ s; (c) $t_3 = 30$ s; (d) $t_4 = 50$ s; (e) $t_5 = 100$ s (Shigorina et al. 2020, under revision).



Water level height above sandstone

What about reality?



Figure 7: Flow through fracture networks and well-known topology/geometry (Rüdiger et al. 2020, under revision).

- Effect of adjacent porous matrix
- Connection between fracture topology/geometry, matrix properties and infiltration dynamics
- Relation to field site experiments?
- Effects of dimension reduction, 2D vs. 3D?

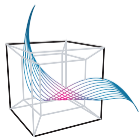
Conclusion

- Fracture networks provide rapid bypass capacities
- Fracture intersections are critical relay points for rapid infiltration
- Transfer function can be obtained/enhanced via small-scale process analysis
- The porous matrix plays a crucial role in the redistribution and large-scale dispersion dynamics
- Field experiments and analogue fracture setups are required to cross-validate findings and explore the quality of analytical abstraction

Stay healthy and see you next year!

—

Questions? Drop me a mail or join our live chat:
Tuesday, 5 May 2020, 08:30–10:15.



www.janneskordilla.org
jkordil@gwdg.de



GEORG-AUGUST-UNIVERSITÄT
GÖTTINGEN



Bundesministerium
für Bildung
und Forschung



Deutsche
Forschungsgemeinschaft



Deutscher Akademischer Austauschdienst
German Academic Exchange Service